Computers and Electronics in Agriculture 70 (2010) 129–134

Contents lists available at ScienceDirect

Computers and Electronics in Agriculture

journal homepage: www.elsevier.com/locate/compag

In-line detection of apple defects using three color cameras system

Zou Xiao-bo[a,*], Zhao Jie-wen[a], Li Yanxiao[a], Mel Holmes[b]

[a] School of Food and Biological Engineering, Jiangsu University, Zhenjiang 212013, China
[b] Procter Department of Food Science, The University of Leeds, Leeds LS2 9JT, United Kingdom

ARTICLE INFO

Article history:
Received 29 July 2008
Received in revised form 18 June 2009
Accepted 26 September 2009

Keywords:
Apple
Defect
Segmentation
Imaging processing

ABSTRACT

Identification of apple stem-ends and calyxes from defects on process grading lines is a challenging task due to the complexity of the process. An in-line detection of the apple defect is developed in this article. Firstly, a computer controlled system using three color cameras is placed on the line. In this system, the apples placed on rollers are rotating while moving, and each camera is capturing three images from each apple. In total nine images are obtained for each apple allowing the total surface to be scanned. Secondly, the apple image is segmented from the black background by multi-threshold methods. The defects, including the stem-ends and calyxes, called regions of interest (ROIs), are segmented and counted in each of the nine images. Thirdly, since a calyx and stem-end cannot appear at the same image, an apple is defective if any one of the nine images has two or more ROIs. There are no complex imaging processes or pattern recognition algorithms in this method, because it is only necessary to know how many ROIs are there in a given apple's image. Good separation between normal and defective apples was obtained. The classification error of unjustified acceptance of blemished apples reduced from 21.8% for a single camera to 4.2% for the three camera system, at the expense of rejecting a higher proportion of good apples. Averaged over false positive and false negative, the classification error reduced from 15 to 11%. The disadvantage of this method is that it could not distinguish different defect types. Defects such as bruising, scab, fungal growth, and disease, are treated as the same.

1. Introduction

China has an annual production of over 20 million tons of apples since 2000. After harvest, they are transported to the packing plant to be tested for various quality attributes that determine their price and destination. The external appearance is one of the most important factors in pricing the apples. Machine vision and imaging processing techniques have been increasingly important for the fruit industry, especially when applied to quality inspection and defect sorting applications (Burks et al., 2005). Automated inspection of apple quality involves computer recognition of good apples and blemished apples based on geometric or statistical features derived from the apple images. Nowadays, mechanical non-destructive devices for in-line measurement of weight, size and color working at high speed (several apples/s), are common in current packinghouses. However, automating the defect sorting process is still a challenging project due to the complexity of the process. One of the biggest difficulties involved in the technology of automated machine vision inspection of fruit defects is how to distinguish the stem-end (stem cavity) and calyx (bloom bottom) from true defects such as bruises, insect damages, and blemishes. Tao and his group have conducted many constructive and fundamental research works to solve this problem, including, image processing (Tao et al., 1995; Ying et al., 2003; Zhu et al., 2007a), structured lighting methods (Tao and Wen, 1999; Wen and Tao, 1997), spectral imaging technology (Cheng et al., 2003; Wen and Tao, 1998; Wen and Tao, 2000) and other techniques (Tao, 1998; Zhu et al., 2007b).

In common systems, the fruits placed on rollers are rotated while moving in-line, and observed by a single charge coupled device (CCD) camera (Abdullah et al., 2006). In this case, the parts of the fruit near the points where the rotation axis crosses its surface (defined as rotational poles) are not observed. Also the identification of apple stem-ends and calyxes from defects by imaging process continues to be problematic (Wen and Tao, 1998).

However, apple defects cause food safety concerns touching the general public and may strongly affect the commodity market. Numerous articles are concerned with the detection of defects on apples. Recently, spectral imaging techniques, such as multi-spectral imaging (Ariana et al., 2006; Blasco et al., 2007; Kleynen et al., 2005; Unay and Gosselin, 2006) and hyper-spectral imaging (Lefcout et al., 2006; Nakajima and Yoshikawa, 2006; Xing et al., 2007), have been employed to detect the defects. Most current computer vision systems used in the automatic quality inspection of food are limited to the visible region (such as normal RGB color) of the electromagnetic spectrum as they tend to imitate the human

* Corresponding author. Tel.: +86 511 88780174.
E-mail address: zou_xiaobo@ujs.edu.cn (Z. Xiao-bo).

0168-1699/$ – see front matter © 2009 Elsevier B.V. All rights reserved.
doi:10.1016/j.compag.2009.09.014

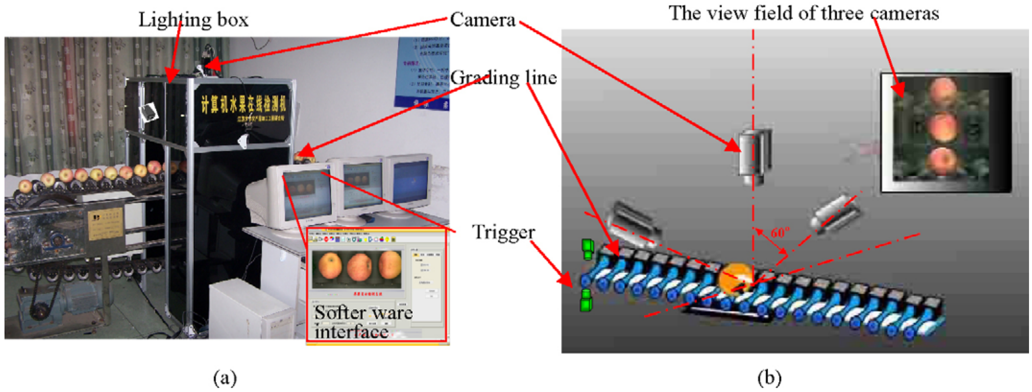

Fig. 1. Hardware system of apple in-line detection: (a) system hardware and (b) schematic of three cameras system.

eye. However, non-visible information, such as that provided by near-infrared (Bennedsen et al., 2005) or ultraviolet regions of the spectrum, can improve the inspection by detecting specific defects or allowing the detection of non-visible damages. Results showed that the contribution of non-visible information can improve the detection and identification of some defects (Mehl et al., 2002; Throop et al., 2005). In these techniques, two steps were performed: (1) hyper-spectral image analysis to characterize spectral features of apples for the specific selection of filters to design the multi-spectral imaging system and (2) multi-spectral imaging for rapid detection of apple defects. Good isolation of scabs, fungal, soil contaminations, and bruises was observed with hyper-spectral imaging using either principal component analysis or the chlorophyll absorption peak. This hyper-spectral analysis allowed the determination of three spectral bands capable of separating normal from defect apples. These spectral bands were implemented in a multi-spectral imaging system with specific band pass filters to detect apple defects (Mehl et al., 2002). These results have shown that the spectral imaging technique is an efficient approach for the detection of defects. However, the spectral imaging technique, as the common system, using only one camera (or two cameras along the direction of the apple sorting line) to scan the surface of fruits is insufficient. This would reduce accuracy of the system. As it may be seen, most researchers did not consider how to manage several images representing the whole surface of the fruit (Leemans, 2004). Generally each image was treated separately and the fruit was classified according to the worse result of the set of representative images.

Among various types of defects, patch-like defects such as bruises, rots and insects bites are the most important ones. These are small, connected areas and generally darker than their surrounding normal surfaces. This paper presents a method for the detection of this type of defects. It is known that the stem-ends and calyxes cannot appear in the same image. Therefore, if there are two or more doubtful ROIs on an apple's image, it may be classified as defective. There are no complex imaging processes or pattern recognition algorithms in this method, because it is only necessary to know how many ROIs there are in a given apple's image. However, the proposed method requires more images to cover the whole surface of the fruit. The objective was to see if less defective apples are accepted if three cameras are used.

2. Materials and methods

2.1. The hardware

The lighting and image acquisition system were designed to be adapted on an existing single row grading machine (prototype from Jiangsu Univ., China). Six lighting tubes (18 W, type 33 from Philips,

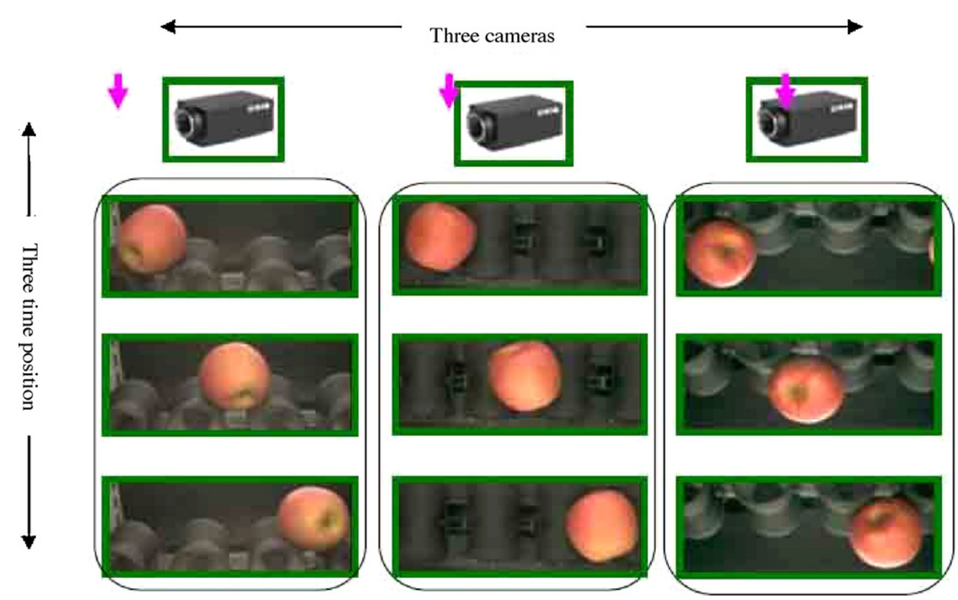

Fig. 2. Trigger grab of nine images for an apple by three cameras at three positions.

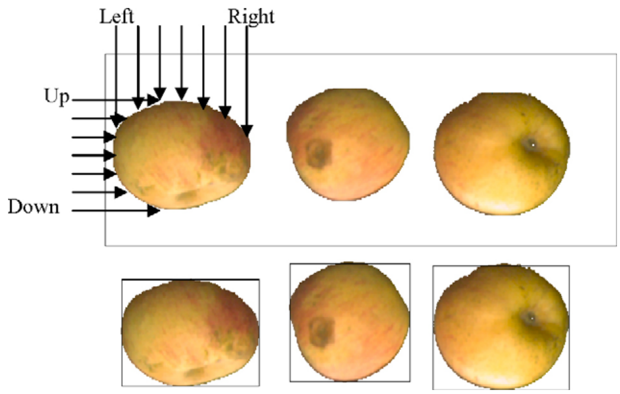

Fig. 3. Single child apple images segmentation.

Netherlands) were placed at the inner side of a lighting box while three cameras (color 3CCD uc610 from Uniq, USA), two having their optical axis in a plane perpendicular to the fruit movement and inclined at 60° with respect to the vertical and one above observed the grading line in the box, as shown in Figs. 1 and 2. The lighting box is 1000 mm in length and 1000 mm in width. The distance between apple and camera is 580 mm, thus there are three apples in the view field of each camera with a resolution of 0.4456 mm per pixel. The images were captured using three Matrox/meteorII digitized frame-grabbers (Matrox, Canada) loaded in three separate computers. The standard image treatment functions were based on the Matrox libraries (Matrox, Canada) with remaining algorithms implemented in C++. A local network was built among the computers in order to communicate results data. The central processing unit of each computer was a Pentium 4 (Intel, USA) clocked at 3.0 GHz. The fruits placed on corn-shaped rollers are rotating while moving. The friction between rollers and the belt on the conveyor rack makes the corn-shaped roller rotate while moving through the field-of-view of the cameras. This was adjusted in such a way that a spherical object having a diameter of 80 mm made a rotation in exactly three images when passed through the view field of camera. The moving speed in the range 0–15 apples per second could be adjusted by the stepping motor.

2.2. Image acquisition and preprocessing

The Matrox digitized frame-grabber supports trigger input from an external trigger when it captures an image. The external trigger is composed of an emitter and an acceptor placed in the grading line as shown in Fig. 1(a). The three frame-grabbers capture images when every roller passes through the trigger. As mentioned above, there are three apples in the view field of each camera, therefore, nine images were grabbed from each apple as shown in Fig. 2.

Image preprocessing includes background segmentation, image de-noise, child image segmentation and sequential image processing.

The background is relatively complicated. To filter the background, multi-threshold methods were performed. That is, the *R*-value in RGB (red-green-blue) and *S*-value in HIS (hue-intensity-saturation) were taken into account. The segmentation values are follows:

$$p(x, y) = \begin{cases} \text{background pixel}: & R < 90 \cup (S < 0.20 \cap R < 200) \\ \text{apple pixel}: & \text{else} \end{cases} \quad (1)$$

Residual noise may be present in the image after the removal of the background, so this paper introduces medial filtering to perform additional filtering. Fig. 3 shows the image after background segmentation and noise reduction.

Given there are three apples waiting for measurement in the field-of-view at most, single apple division has become an inevitable operation. The minimum enclosing rectangle of each single apple was used to divide the initial image into three child images as shown in Fig. 3.

Continuous image grabbing therefore produces a group of sequential images, with related information existing between each single child image. In the work conducted in this paper, the processing design of the sequential images is analyzed for various configurations (e.g. apple present or not). A two-dimensional array *R* was used to represent the three child images as shown in Fig. 4 to draw following three conclusions.

Firstly, among the three child images, the left child image represents an apple in position 1, the middle image represents an apple in position 2, and the right child image represents an apple in position 3. These rules do not change when the trigger grabbing times increase.

Secondly, the sub-numbers of array *R* of No. 6 (the times of trigger grabbing $I = 6$) apple is the same as those of No. 3 (the times of trigger grabbing $I = 3$) apple, and there is a cycle beginning. The cycle variable: $X = I \bmod 3$.

Third, it is a special case when $I = 1$ or $I = 2$. The cycle variable should be:

$$X = (I - 1) \bmod 3.$$

The information captured for a given apple in the array *R* was saved when it appeared three times, otherwise, it will be overwritten by the information of following apples. ADO (ActiveX Data Objects) was used to save the information into a database.

2.3. Blemish (or defects) segmentation and recognition

There exist several image analysis methods for defect detection, including global grey-level or gradient thresholding, simple background subtraction, statistical classification and color classification (Yang, 1994). Blemish segmentation is a difficult problem in image analysis, because various types of blemishes with different size and extent of damage may occur on fruit surfaces. If a blemish appears as very a dark mark on a fruit surface, a simple thresholding of grey-level intensity of reflected light may allow a direct segmentation of the blemish. However, in most cases, the light reflectance from both blemished and non-blemished surfaces varies considerably, and it is impossible to set a single threshold value for the segmentation. For example, a patch of good surface with a relatively dark color can have similar reflectance as a slightly discolored blemish on a light colored surface. In this case, the thresholding method will fail.

An image analysis scheme for accurate detection of fruit blemishes proposed by (Qingsheng Yang, 1996) is used in this study. The detection procedure consists of two steps: initial segmentation and refinement. In the first step, blemishes are coarsely segmented out with a flooding algorithm and in the second step an active contour model, i.e. a snake algorithm, is applied to refine the segmentation so that the localization and size accuracy of detected blemishes is improved. However, Yang's algorithms were tested on monochrome images of mono-color fruits. Here the images are color images of bi-color fruit.

The appearances of calyxes and stem-ends are also like the patch-like defects, these patches were defined as ROIs. The ROIs are generally darker than their surrounding non-defective surfaces, and in image grey-level landscapes they usually appear as significant concavities using the concept of topographic representation.

The median filtering process mentioned in image preprocessing improved the success of the flooding algorithm. This smoothing

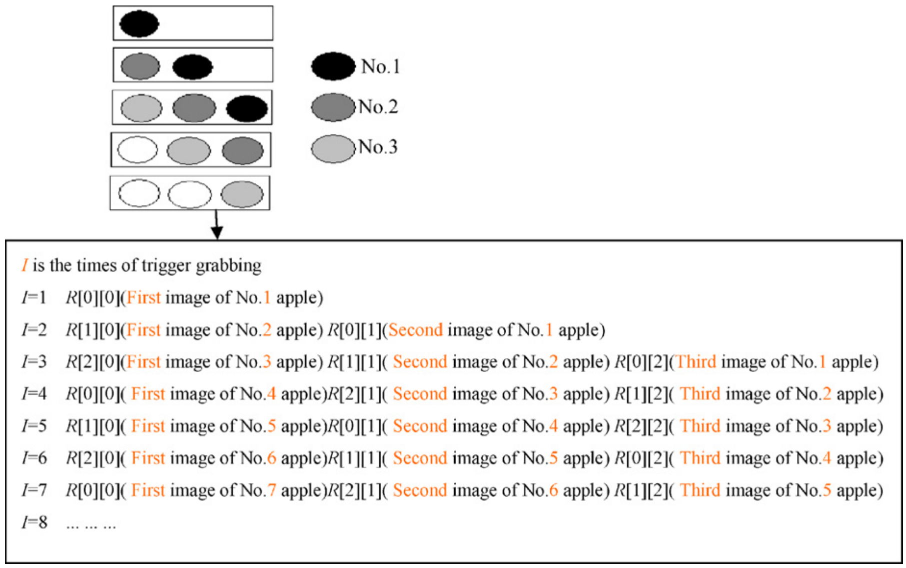

Fig. 4. Sequential image and the single child image representation.

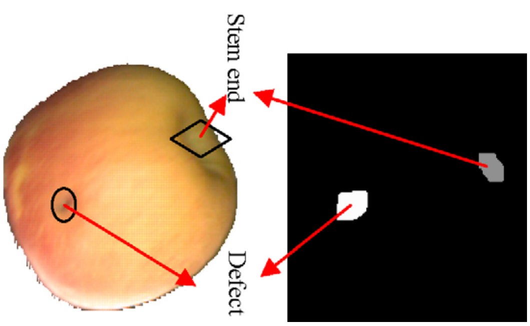

Fig. 5. Precise segmentation of ROIs area.

naturally distorts the grey-level surface and thus has a drawback effect that the segmented areas are larger than those that we see. Since the size of a ROI is important for grade decision-making, a refinement of the defect detection is necessary. A closed loop snake has been implemented to improve the boundary localization of detected ROI (Yang, 1994). Then, the minimum enclosing rectangle of each single ROI was used to measure the size of ROI. If the dimensions of the rectangle exceed 5 pixels (0.4456 mm per pixel), the measured ROI area is take into account. The R channel signals were used to detect the defects, because the tests for sample apple R channel images have shown better results than other channel images.

The defect recognition steps are as follows.

Firstly, the number of ROIs is counted in each single child apple image.

Secondly, logical recognition rules were developed. That is, since calyx and stem-ends could not appear in a single child image at the same time, an apple is defective if any one of its nine images has two or more ROIs. Fig. 5 shows an example of an apple image that has two ROIs.

Thirdly, the defect detection mentioned above is all based on the data acquisition using three computers, consequently, an apples characteristic parameters is formed by integration into a single source. One of the three computers is server; the other two

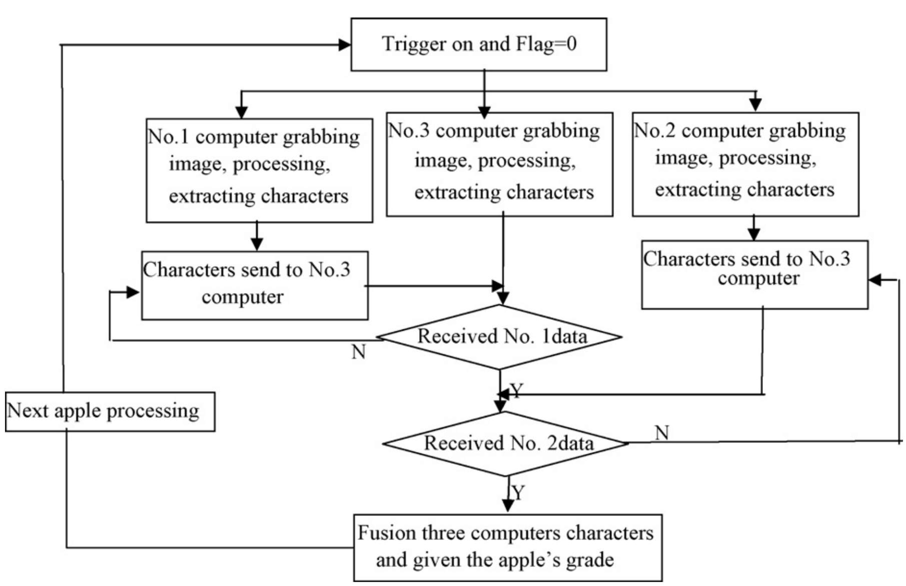

Fig. 6. Three computers image processing and synchronization online grading.

Table 1
The results obtained by the three color cameras grading line.

True groups Graded in	Accepted(Apples without defects, 199 apples)		Rejected(Apples with defects, 119 apples)
Accepted (174 apples)	169		5
Rejected (144 apples)	30		114
Classification error (%)	15.07%		4.2%
Global classification error (%)		11%	

Table 2
The results obtained by the two inclined color cameras grading line.

True groups Graded in	Accepted(Apples without defects, 199 apples)		Rejected(Apples with defects, 119 apples)
Accepted (189 apples)	172		17
Rejected (129 apples)	27		102
Classification error (%)	13.56%		14.3%
Global classification error (%)		13.8%	

Table 3
The results obtained by the only one camera (the above camera) grading line.

True groups Graded in	Accepted(Apples without defects, 199 apples)		Rejected(Apples with defects, 119 apples)
Accepted (203 apples)	177		26
Rejected (115 apples)	22		93
Classification error (%)	11%		21.8%
Global classification error (%)		15.1%	

computers are customers. Fig. 6 shows the data exchange and synchronization during in-line grading.

Since nine images are sufficient to encompass the whole surface of the apple, any defects in the surface can be detected by this method. The disadvantage of this method is that it could not distinguish different defect types. Defects of apples, such as bruising, scab, fungal growth, and disease, are treated as equivalent. The apples were then graded to reject or accept.

2.4. Apples

All the apples used in this experiment were selected and came from the same grower. 318 “fuji” apples were used in only one experiment and each fruit was thus presented only once to the machine to avoid any additional bruises. The apples were classified into two classes: accepted (199 apples) and rejected (with blemish, 119 apples).

3. Results and discussion

Figs. 1 and 2 show the hardware system of apple in-line detection and the trigger grabbing of nine images from an apple by the system. Furthermore, if the diameters of apple vary from 60 mm to 110 mm, the system still can cover the whole surface by the three image-triplets. After background segmentation, noise reduction, child image segmentation and sequential image processing, initial segmentation results for an apple are displayed in Fig. 5. The segmented ROIs were highlighted with dark and bright borders. Both the defect and the stem-end were detected.

The proposed system has been tested with a laboratory three CCD cameras system for “fuji” apples. The results obtained by the three color cameras grading line are given in Table 1. The total error rate reached 11% mostly occurring in the accepted batch. When these errors were analyzed, half of the errors were apples with over-segmentation of healthy tissue and especially in the tissue near the boundaries in the defect segmentation processing. The other half was attributed to two reasons. Firstly, spot blush on the surface of good apples is segmented as defective and the apple is classified into the rejected class. As the flooding algorithm used by Yang (1994) was designed to detect “catchments basins”, i.e. areas with a lower luminance, large spot blushes were easily segmented as ROI. Secondly, errors occur because apples with defects are accepted, i.e. false positives. These errors were due to defects that are difficult to segment such as russet and bruises. Those defects were present near the stem-ends and calyxes of apples. They have almost the same appearance as the russet around the stem-end and, because of the proximity in position and appearance, were probably confused with the latter. The defect is localized together with the stem-end and counted as one ROI. Therefore, this apple was segmented as a good one.

Comparing different configurations, the results of a sorting line with only one camera (the above camera) and sorting line with the two inclined cameras, are shown in Tables 2 and 3. With one camera, 21.8% of the apples with no defects are misclassified (i.e. they are accepted), whereas this number reduces significantly from 14.3% with two cameras to 4.2% with three cameras. However, at the same time, the classification error for good apples increases from 11% for one camera (3 images), via 13.56% for two (6 images) to 15.07% for three cameras (9 images). This is mainly caused by the information loss. A statistic test was carried out for the loss of information when different numbers of cameras were utilized in the sorting line. 15–20% of the apple’s surface cannot be observed from the three images obtained by the single overhead camera. 5–10% of the apple surface information will be lost using two inclined cameras. After statistic analysis, the individual images (child images) obtained by three CCD cameras resulted in a probability for a defect to be present alone in one child image alone as 28.4% after testing 318 apples ($318 \times 9 = 2862$ child images). However, the nine images obtained by the three cameras could cover the whole surface of the apple. With defective apples, more images provide more opportunity to detect the defects, thus leading to a lower classification error. With good apples, more images means a change to classify spot blush as defect, and hence more will be misclassified. This is caused by the defect detection algorithm. There are defects that are not darker than their surrounding and could thus not be recognized. On the other hand, some parts of the fruit are darker than their surroundings. There are also other reasons for errors. Less defective apples in the accepted bin give higher prices that can compensate for the slightly increase loss of good apples. With three cameras, the class of “accepted” apples now has 174 apples, of which 5 still have defects (i.e. some 2.87%). Whereas with one camera the accepted bin has 203 apples, but with 26 defective ones (i.e. some 13%).

4. Conclusions

The grading of apples into quality classes is a complex task. A three color CCD cameras classification system was investigated in this paper. Multi-threshold method was proposed to segment the apple image from black background. Patch-like defects including calyxes and stem-ends, which defined as ROIs, were identified by Yang's algorithm (Qingsheng Yang, 1996). When two or more ROIs are identified, the apple was classified into the reject class. The experimental results demonstrated that less bad apples appear in the "accepted" bin, but at the same time more good apples end up in the "rejected" bin. The global classification error for the in-line sorting using three cameras was the lowest. There were fewer rejected apples misclassified into the accepted category. In future work, the defect detection algorithm should be improved to overcome the expense of rejecting such a high proportion of good apples. Enhancement of the grading process should come from every stage, and particularly, from the image acquisition stage. Indeed, better light repartition and use of specific wavelengths revealing high contrast between defects and healthy tissue will enhance the global machine performances.

Acknowledgements

This work is supported by "Natural Science Foundation of China" and "863 high-tech fund of China" Fund. We also wish to thank many of our colleagues for many stimulating discussions in this field.

References

Abdullah, M.Z., Mohamad-Saleh, J., Fathinul-Syahir, A.S., Mohd-Azemi, B.M.N., 2006. Discrimination and classification of fresh-cut star fruits (Overheat parabola L.) using automated machine vision system. Journal of Food Engineering 76 (4), 506–523.

Ariana, D., Guyer, D.E., Shrestha, B., 2006. Integrating multispectral reflectance and fluorescence imaging for defect detection on apples. Computers and Electronics in Agriculture 50 (2), 148–161.

Bennedsen, B.S., Peterson, D.L., Tabb, A., 2005. Identifying defects in images of rotating apples. Computers and Electronics in Agriculture 48 (2), 92–102.

Blasco, J., Aleixos, N., Gomez, J., Molto, E., 2007. Citrus sorting by identification of the most common defects using multispectral computer vision. Journal of Food Engineering 83 (3), 384–393.

Burks, T., Villegas, F., Hannan, M., Flood, S., Sivaraman, B., Subramanian, V., Sikes, J., 2005. Engineering and horticultural aspects of robotic fruit harvesting: opportunities and constraints. Horttechnology 15 (1), 79–87.

Cheng, X., Tao, Y., Chen, Y.-R., Luo, Y., 2003. NIR/MIR dual-sensor machine vision system for online apple stem-end/calyx recognition. Transactions of the American Society of Agricultural Engineers 46 (2), 551–558.

Kleynen, O., Leemans, V., Destain, M.F., 2005. Development of a multi-spectral vision system for the detection of defects on apples. Journal of Food Engineering 69 (1), 41–49.

Leemans, V., Destain, M.-F., 2004. A real-time grading method of apples based on features extracted from defects. Journal of Food Engineering 61, 83–89.

Lefcout, A.M., Kim, M.S., Chen, Y.-R., Kan, S., 2006. Systematic approach for using hyperspectral imaging data to develop multispectral imagining systems: detection of feces on apples. Computers and Electronics in Agriculture 54 (1), 22–35.

Mehl, P.M., Chao, K., Kim, M., Chen, Y.-R., 2002. Detection of defects on selected apple cultivars using hyperspectral and multispectral image analysis. Applied Engineering in Agriculture 18 (2), 219–226.

Nakajima, T., Yoshikawa, K., 2006. A discrimination model for fruit rot in satsuma mandarins using spectral imaging and multivariate analysis—(Discrimination system for rot in satsuma mandarins using spectral imaging—Part 2). Journal of the Japanese Society for Food Science and Technology-Nippon Shokuhin Kagaku Kogaku Kaishi 53 (11), 561–565.

Qingsheng Yang, J.A.M., 1996. Accurate blemish detection with active contour models. Computers and Electronics in Agriculture 14, 77–89.

Tao, Y., 1998. Closed-loop search method for on-line automatic calibration of multi-camera inspection systems. Transactions of the ASAE 41 (5), 1549–1555.

Tao, Y., Heinemann, P.H., Varghese, Z., Morrow, C.T., Sommer III, H.J., 1995. Machine vision for color inspection of potatoes and apples. Transactions of the ASAE 38 (5), 1555–1561.

Tao, Y., Wen, Z., 1999. Adaptive spherical image transform for high-speed fruit defect detection. Transactions of the ASAE 42 (1), 241–246.

Throop, J.A., Aneshansley, D.J., Anger, W.C., Peterson, D.L., 2005. Quality evaluation of apples based on surface defects: development of an automated inspection system. Postharvest Biology and Technology 36 (3), 281–290.

Unay, D., Gosselin, B., 2006. Automatic defect segmentation of 'Jonagold' apples on multi-spectral images: a comparative study. Postharvest Biology and Technology 42 (3), 271–279.

Wen, Z., Tao Y., 1997. Intensity Compensation for On-line Detection of Defects on Fruit. San Diego, CA, United States, pp. 474–481.

Wen, Z., Tao, Y., 1998. Dual-wavelength Imaging for On-line Identification of Stem-ends and Calyxes. San Diego, CA, United States, pp. 249–253.

Wen, Z., Tao, Y., 2000. Dual-camera NIR/MIR imaging for stem-end/calyx identification in apple defect sorting. Transactions of the ASAE 43 (2), 449–452.

Xing, J., Jancsok, P., De Baerdemaeker, J., 2007. Stem-end/calyx identification on apples using contour analysis in multispectral images. Biosystems Engineering 96 (2), 231–237.

Yang, Q., 1994. Approach to apple surface feature detection by machine vision. Computers and Electronics in Agriculture 11 (2–3), 249–264.

Ying, Y., Jing, H., Tao, Y., Zhang, N., 2003. Detecting stem and shape of pears using Fourier transformation and an artificial neural network. Transactions of the ASAE 46 (1), 157–162.

Zhu, B., Jiang, L., Luo, Y.G., Tao, Y., 2007a. Gabor feature-based apple quality inspection using kernel principal component analysis. Journal of Food Engineering 81 (4), 741–749.

Zhu, B., Jiang, L., Tao, Y., 2007b. Automated 3D Surface Reconstruction and Analysis of apple Near-Infrared data for the application of apple stem-end/calyx identification. Minneapolis, MN, United States, p. 14.